Journal of Statistical Physics, Vol. 73, Nos. 1/2, 1993

Langevin Dynamic Simulation of Hysteresis in a Field-Swept Landau Potential

Mangal C. Mahato[1] **and Subodh R. Shenoy**[1]

Received February 5, 1993

Numerical simulations are done of Langevin dynamics for a uniform-order-parameter, field-swept Landau model, $\Phi = -|a/2|m^2 + |b/4|m^4 - mh(t)$, to study hysteresis effects. The field is swept at a constant rate $h(t) = h(0) + \dot{h}t$. The stochastic jump values of the field $\{h_J\}$ from an initially prepared metastable minimum $m(0)$ are recorded, on passage to a global minimum $m(\tau)$. The results are: (a) The mean jump $\bar{h}_J(\dot{h})$ increases (hysteresis loop widens) with $\dot{h}$, confirming a previous theoretical criterion based on rate competition between field-sweep and inverse mean first-passage time $\langle \tau \rangle$ (FPT); (b) The broad jump distribution $\rho(h_J, \dot{h})$ is related to intrinsically large FPT fluctuations $(\langle \tau^2 \rangle - \langle \tau \rangle^2)/\langle \tau^2 \rangle \sim O(1)$, and can be quantitatively understood. Possible experimental tests of the ideas are indicated.

KEY WORDS: Hysteresis; overshoot phenomena; Langevin simulation; time sweep of control parameter; first passage times.

1. INTRODUCTION

Hysteresis or overshoot phenomena occur in a diverse range of systems, such as magnets,[1] glassy melts,[2,3] and optically bistable devices.[4] When an external control parameter is swept, the system does not respond linearly and instantaneously, but overshoots past the reversible transition path. On repeated cycling, back and forth, the overshoots trace out a closed hysteresis curve.

An example of a temperature-induced overshoot is the supercooling of a liquid melt past its crystallization temperature. For sufficiently large cooling rate $|\dot{T}|$ and a large undercooling, glass may be formed. Clearly, hysteresis may have kinetic aspects that depend on intrinsic time scales and external control-parameter sweep rates.

[1]School of Physics, University of Hyderabad, Hyderabad-500 134, India.

0022-4715/93/1000-0123$07.00/0

Approaches to hysteresis, as opposed to purely relaxational studies of first-order kinetics, may be divided into at least three broad categories.

(a) Phenomenological free energies $F(m, h)$ with physically motivated nonlinearities or inhomogeneities[5–7] giving rise to a nonlinear (and deterministic) $\bar{m}(h)$. One could also include switching rules[8] based on these ideas.

(b) Numerical solution of coupled deterministic equations for the order parameter and correlation function, obtained from averaging time-dependent Ginzburg–Landau equations, with noise, and with sinusoidal drives $h(t) = H_0 \sin(\Omega t)$. These hysteresis investigations[9,10] go beyond previous, purely relaxational, calculations.

(c) Hysteresis based on Langevin kinetics,[11–18] (or Monte Carlo simulations[19]) in particular rate competition between sweep rates and decay/relaxation rates.

Within the last-mentioned category, a detailed general criterion for hysteresis has been developed by Agarwal and Shenoy[15,16] based on the first-passage time (FPT) formalism.[20] The starting point is a Langevin equation for the order parameter $m(t)$, and the FPT equation derived from it includes competing deterministic and stochastic forces. The criterion states that for hysteresis to occur, the field-sweep rate $\dot{h}$ should exceed a minimum $\dot{h}_{\min}(h)$ set by the field-dependent times scales of the system: $\dot{h} \geqslant \dot{h}_{\min}(h)$. The equality denotes the failure of hysteresis, and defines a theoretical (mean) jump value $h = \bar{h}_J$.

In this paper (which is a longer version of a conference presentation[18]) we do a numerical simulation of a driven Langevin model, without averaging or truncation, to study "experimentally" the phenomenon of hysteresis. The model is one of the simplest possible that can undergo a first-order transition, namely a uniform-m Landau free energy with a double well,

$$\Phi \equiv -\frac{|a|}{2} m^2 + \frac{|b|}{4} m^4 - mh(t) \tag{1.1}$$

The model has recently been found[17] to have a physical realization through a silica grain hopping between two optical traps of high field intensity. This model can be also viewed as representing a magnetic "domain" of finite size of magnetization m. The control parameter is an external magnetic field, linearly swept at a constant rate $\dot{h}$, which plays a central conceptual role:

$$h(t) = h(0) + \dot{h}t \tag{1.2}$$

The Langevin equation is solved for $m(t)$ for fixed $\dot{h}$. The data collected for N independent repeated runs for a given $\dot{h}$ are the (stochastic) field values

$\{h_J\}$ at which a "jump" occurs to the globally stable minimum (Fig. 1). The "jump field" thus is not a single value even for $N \to \infty$, but is a distribution.

Comparison is made between the theoretical[12, 15, 16] $\bar{h}_J(\dot{h})$ and the mean value from experimental data $\{h_J\}$. The faster the sweep, the greater is the overshoot. However, we do not find a simple universal-exponent power-law dependence[10, 19, 24, 25] on the sweep rate. Fluctuations, described by the distribution $\rho(h_J; \dot{h})$, can be theoretically related to the *intrinsically* large fluctuations in the first-passage time, where, for $\dot{h} = 0$, $(\langle \tau^2 \rangle - \langle \tau \rangle^2)/\langle \tau \rangle^2 \approx O(1)$. A quantitative understanding of hysteresis in a Landau–Langevin model is thus obtained that may have a more general relevance.

Our work differs from others[9, 10, 19, 24, 25] in certain respects.

The conceptual advantage of a linear $h(t)$ sweep is that the sweep rate $\dot{h}$ is a constant, independent of both time and initial value $h(0)$. (A repetitive cycling would involve a piecewise constant $\dot{h}$.) This focuses on the essential picture of hysteresis as rate competition. By contrast, a cosine sweep $h(t) = h(0)\cos(\Omega t)$ has a more complex sweep rate that depends on initial values and varies at every instant of the sweep.

The advantage of using ai first-passage-time formulation to estimate metastable lifetimes is that while the mean value is essentially the inverse Kramers rate,[21] the FPT formalism is more powerful, in that it can describe lifetime fluctuations, which turns out to be important.

The advantage of using a Langevin simulation is that it is a computer

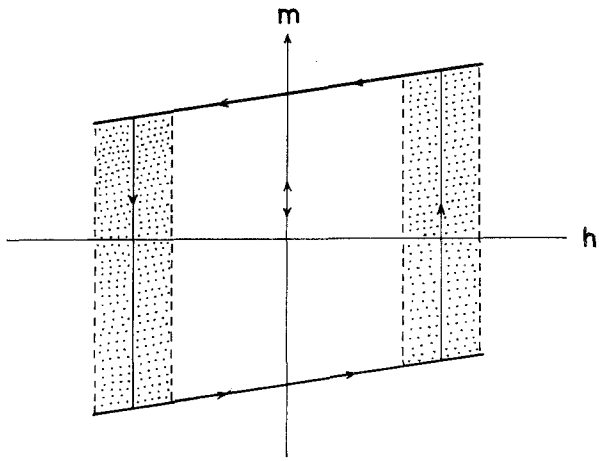

Fig. 1. Schematic mean order parameter $\bar{m}$ versus field h. For $\dot{h} = 0$ there is a reversible jump at $h = 0^+$ or 0^-; for $\dot{h} \neq 0$, a hysteresis loop with a mean jump at $(\bar{h}_J(\dot{h})$ and a scatter under repeated runs.

experiment directly recording the interplay between the stochastic jump and the deterministic sweep that underlies hysteresis.

We now briefly consider some background to this work. The early phenomenological approaches to magnetization hysteresis have already been reviewed elsewhere.[5–7,10] The work by Barker *et al.*,[5,6] in particular, considers a model of noninteracting uniform-m domains and a distribution of jump fields yielding hysteresis curves on averaging.

Within numerical work, Binder[22] has considered nonequilibrium magnetization decay in Ginzburg–Landau models, introducing a nonlinear relaxation function based on deviation from eventual $t \to \infty$ values. Paul *et al.*[23] have considered the relaxation of mean-field, finite-volume Ising systems described by a master equation and also evaluated mean first-passage times for metastable decay. Mazenko and Zannetti[9] considered relaxation in multicomponent $(\sum_{i=1}^{n} \psi_i^2(r))^2$ models with Langevin dynamics. They averaged over random forces and solved the coupled order-parameter and correlation-function equations. Rao *et al.*[10] included a sinusoidally cycled field $h(t) = H_0 \sin(\Omega t)$ to consider hysteresis effects in this model. A principal result was the scaling of the hysteresis loop area A with the amplitude H_0 and frequency Ω as $A \propto H_0^{\alpha} \Omega^{\beta}$. The exponents α and β for this system were found to be $\alpha = 0.66 \pm 0.05$ and $\beta = 0.33 \pm 0.03$ over a frequency range extending over three decades. A cell dynamical simulation was done for an $n = 1$, $2D$, $(\phi^2)^2$ model by Sengupta *et al.*,[24] who obtained $\alpha = 0.47 \pm 0.02$ and $\beta = 0.40 \pm 0.01$. Dhar and Thomas[25] find $\alpha = \beta = 1/2$ in an n-vector model, for large n. Ising model simulations[19] show $\alpha = \beta = 0.36$ in a low frequency limit. Jung *et al.*[26] studied the overdamped (deterministic) dynamics of a particle in a bistable $n = 1$ model with a quadratic double well and a sinusoidal driving force. Their study naturally overestimated the area A, since jumps occur only after the spinodal point, when barriers vanish. They found $\alpha = \beta = 2/3$.

Turning to hysteresis criteria based on rate competition, the naive early estimate is as follows.[11,12] To observe hysteresis, the field sweep rate $\dot{h}$ should be faster than the system decay rate from the initial state to the energetically favorable final state. Various forms of this intuitive idea are all essentially equivalent to $\dot{h} > \tau_{\text{decay}}^{-1}$, where τ_{decay} is the characteristic decay time of the system. Skripov and Skripov[11] suggested this criterion on physical grounds (spinodal decay model). Gilmore[12] suggested that τ_{decay} could be estimated by the mean FPT.

Agarwal and Shenoy[15,16] obtained a more detailed hysteresis criterion, based on rate competition, with important prefactors to the

[2]Alternative definitions of the absorbing boundary are the top of the barrier (m_3 in ref. 15) or some fraction into the globally stable well.[3]

decay rate $\tau_{\text{decay}}^{-1} = \langle \tau \rangle^{-1} \equiv T_P^{-1}$, which depends[2] on the $\bar{m}_3(h)$ boundary defining "passage" and varies with h. Since the main concern involves comparison of *rates* of various processes, the external field was chosen to be linearly varying with time, for simplicity. (The linear variation of the sweeping field is like the temperature sweeps used in the undercooling that precedes the glass transition.) Since the FPT formalism can be generalized[15,27] to n dimensions, the rate-competition hysteresis criterion is not restricted to the single-component case, but can be applied, in principle, to multicomponent[16] or spatially varying order parameters.

The plan of the paper is as follows. In Section 2 the model and method of solution are described and the results presented. Mean jump values $\bar{h}_J(\dot{h}; D)$ are compared with theoretical predictions. In Section 3 theoretical distributions $\rho(h_J; \dot{h})$ are derived and compared with the $\{h_J\}$ histogram from numerical simulation. Section 4 considers averages over independent domains, yielding m–h curves analogous to those in magnetic materials. Finally, Section 5 presents a summary of our results and a discussion. An Appendix gives the justification for the choice of the time discretization step used in the simulations.

2. LANGEVIN DYNAMICS, MEAN JUMP VALUES, AND HYSTERESIS CRITERION

The (overdamped) Langevin dynamics for the magnetization m is described by

$$\frac{dm}{dt} = -\frac{\delta \Phi}{\delta m} + \hat{f}(t) \tag{2.1}$$

where time t is appropriately scaled to be dimensionless. Here $\langle \hat{f}(t) \rangle = 0$ and $\langle \hat{f}(t)\, \hat{f}(t') \rangle = 2D\delta(t-t')$, where D is the diffusion constant, taken to be independent of m. The potential

$$\Phi = -\frac{|a|}{2} m^2 + \frac{|b|}{4} m^4 - mh(t) \tag{2.2}$$

has two minima at $\bar{m}_1(h), \bar{m}_2(h)$, separated by a maximum at $\bar{m}_3(h)$ (Fig. 2). $|a|$, $|b|$, and D are dimensionless. The model may be viewed as a finite-volume single magnetic "domain" with the volume absorbed in the constants. For $h=0$, $\bar{m}_1(0) = -\bar{m}_2(0)$, and in thermodynamic equilibrium, a reversible first-order transition ($\bar{m}_1 \to \bar{m}_2$) occurs for $h = 0^+$, i.e., in infinite time. For $h = \pm h_c = \pm 2(|a|/3|b|)^{3/2}$, at the spinodal points, one of the wells merges with the maximum and disappears.

We consider linearly swept fields

$$h(t) = h(0) + \dot{h}t \tag{2.3}$$

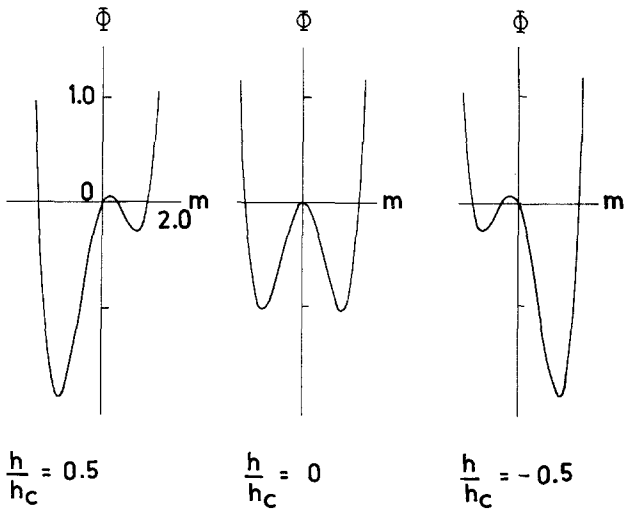

Fig. 2. Free energy $\Phi(m)$ for various values of field h.

where for a constant $\dot{h} \neq 0$ a nonequilibrium state results, and $\dot{h}$ is independent both of time and field. The field is swept until the jump at $h = h_J$ takes place, and the system is then initialized again. Thus we concentrate on understanding an overshoot; the full sawtooth $h(t)$ cycling is built up of these successive overshoots, and will be considered elsewhere.

In a mechanical analogy, the state is a "particle" in a potential well of (2.2) that remains carried along in the metastable well $\bar{m}_1$ till the random force $\hat{f}(t)$ finally kicks it over the changing barrier $\bar{m}_3(t)$, with a roll down to the final globally-stable state $\bar{m}_2$. The passage time T_P includes both hopover and rolldown components (see footnote 2) in our definition of "passage." The FPT in the one-dimensional case, such as (2.2), is exactly soluble,[15,20] as an integral over the stationary distribution $e^{-\Phi/D}$.

The Langevin equation (2.1) is solved numerically by discretizing time $t \to t_n = n\delta t$, with the random force $\hat{f}(t)$ chosen from a Gaussian distribution in each time step δt (see Appendix). The constants are chosen as $a = 2$, $b = 1$. The field $h(t)$ varies as in (2.3), as the simulation proceeds in time. The stochastic jump values $\{h_J\}$ of field $h(\tau)$ when a "jump" from an initial $\bar{m}_1(0)$ to a final $\bar{m}_2(\tau)$ occurs are recorded for N repeated runs. Mean values $\bar{h}_J(\dot{h})$ and jump distribution $\rho(h_J; \dot{h})$ are calculated for various values of diffusion constant $D = 0.2$, 0.5 and sweep rate $\dot{h}/h_c = 0.005$, 0.01, 0.05, 0.1. The optimum value of δt for our calculation is chosen to be $\delta t = 0.001$ (see Appendix), which is small enough for less than 5% deviation from the benchmark of exact theoretical mean FPT values, and large enough for reasonable run times (hours) on a MicroVax II. The number of

runs N is chosen such that the mean FPT values T_P are reproducible to nearly 1% between any runs; typically, $N \sim 1000$.

For completeness, we now outline the theoretical estimates made previously[15,16] and obtain certain simple limits.

In qualitative terms, the jump at h_J occurs when the sweep rate $\dot{h}$ is overtaken by the increasing decay rate as the metastability barrier decreases with $\dot{h}$. As previously noted, this simple estimate[11] is

$$\dot{h} \geqslant \tau_{\text{decay}}^{-1} \tag{2.4}$$

where the decay rate τ_{decay}^{-1} can be[12,15,16] taken to be the inverse mean first passage time T_P^{-1}. This rough criterion has been improved upon,[15,16] and may be stated as follows. For hysteresis to occur, the control parameter drags the metastable peak of the probability distribution

$$P_0(\bar{m}_1(h(t)), h(t)) \equiv \exp^{[-\Phi(\bar{m}_1, h)/D]}$$

at a rate $|\dot{P}_0/P_0| \approx |\dot{h}\,\delta(\Phi/D)/\delta h|$ that must be faster than the *net* rate of decay of the metastable well. This net rate of metastable decay is the difference of the forward decay $\bar{m}_1 \to \bar{m}_2$ and the reverse decay $\bar{m}_2 \to \bar{m}_1$ to and from the stable state. This is estimated by the difference in the inverse first-passage times $T_{P\downarrow}^{-1}(h) - T_{P\uparrow}^{-1}(h)$. Thus, for hysteresis to occur, one must sweep fast enough to outrace the decay,

$$\dot{h} \geqslant \dot{h}_{\min}(h) = \left| \frac{\delta \Phi/D}{\delta h} \right|^{-1} [T_{P\downarrow}^{-1}(h) - T_{P\uparrow}^{-1}(h)] \tag{2.5}$$

As h increases, the net decay rate increases, since $T_{P\downarrow}$ decreases with decreasing barrier and the inequality is eventually violated. The mean jump value $\bar{h}_J(\dot{h}, D)$ at the breakdown of the hysteresis condition inequality is roughly estimated as

$$\dot{h} = \dot{h}_{\min}(\bar{h}_J) \tag{2.6}$$

Ideally, one would like to use a mean first-passage time for a *moving*-boundary case. Since this is not known, in general, we use the $\dot{h} = 0$ first-passage times $T_{P\downarrow}(h)$, $T_{P\uparrow}(h)$ at the instantaneous h value in (2.5) above. Implicit in this is the assumption that the nonequilibrium state rapidly reequilibrates to, and follows, the moving minimum after each unsuccessful passage attempt. This "adiabatic following" condition yields the upper bracket $\dot{h}_{\max}(h) > \dot{h}$ of a "hysteresis window"[15,16] for $\dot{h}$, as mentioned later.

For the high-barrier/weak-noise limit, the FPT expression given in the Appendix can be expanded in a sharp-peaking limit as

$$T_{P\downarrow}^{-1} \approx \pi^{-1}|\omega_1\omega_3|^{1/2} \exp\{-[\Phi(\bar{m}_3)-\Phi(\bar{m}_1)]/D\}$$
$$T_{P\uparrow}^{-1} \approx \pi^{-1}|\omega_2\omega_3|^{1/2} \exp\{-[\Phi(\bar{m}_3)-\Phi(\bar{m}_2)]/D\} \tag{2.7}$$

For a very slow sweep rate $\dot{h}$, (2.6) is expected to be satisfied for a small h_J—jumps occur with only a small overshoot. In this limit $h_J/h_c \ll 1$ and $h\bar{m}_1/D \ll 1$, from (2.5) and (2.7) we get

$$\bar{h}_J \simeq \frac{\dot{h}}{2\omega} e^{+|a|^2/4|b|D} \tag{2.8}$$

where $\omega = |\omega_1\omega_3|^{1/2}$. For fixed D, the mean jump value moves out linearly with sweep rate, $\bar{h}_J \propto \dot{h}$. For faster sweep rate, however, the variation of $\bar{h}_J$ should become slower than linear in $\dot{h}$ (roughly, $\dot{h} \sim e^{-h}$, so $h_J \sim \ln \dot{h}$). As the sweep rate is gradually increased, the hysteresis loop is expected to widen, at first rapidly, and then more slowly. Further, for fixed $\dot{h}$, the jump value $\bar{h}_J$ (and therefore the hysteresis loop area) decreases with increasing diffusion constant D. Jumps aided by increasing D occur earlier, because

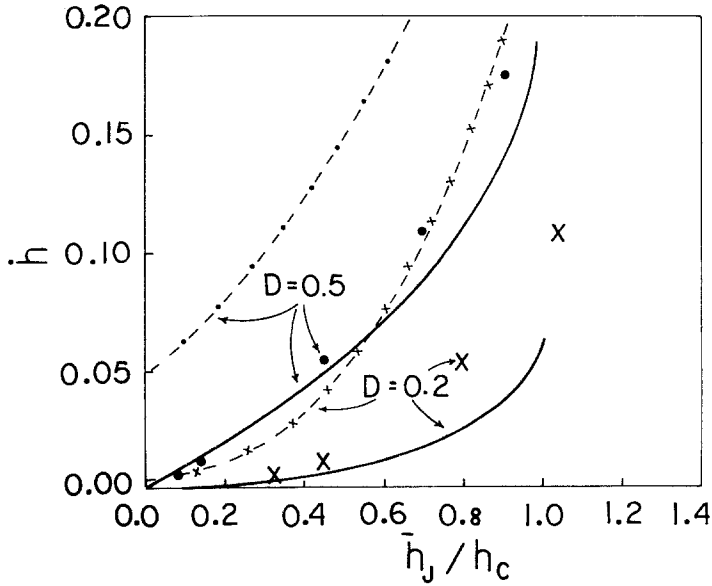

Fig. 3. Mean jump $\bar{h}_J(\dot{h}, D)$ versus $\dot{h}$ for $D = 0.2$ (solid crosses ×) and 0.5 (solid circles ●), showing a widening of the hysteresis loop with sweep rate. Thick solid lines are the theoretical jump curves $\dot{h}_{\min}(h, D)$ of (2.5). Dash-cross ($D = 0.2$) and dash-dot ($D = 0.5$) lines are the alternative jump criterion of (2.4).

the inequality (2.5) is violated sooner. These detailed predictions can be compared to numerical data.

Figure 3 shows the theoretical jump limit $\dot{h}_{\min}$ of (2.5) (thick lines) versus h for two values of $D = 0.2, 0.5$. The vertical axis denotes "rates" and a constant $\dot{h}$ is then a horizontal line whose intersection yields the theoretical $\bar{h}_J$ of (2.6). Note that for $\dot{h} = 0$ one gets the thermodynamic "Maxwell construction" or reversible transition, with no hysteresis as $\bar{h}_J = 0$. Figure 3 shows the numerical simulation data $(\dot{h}, \bar{h}_J)$ for $D = 0.5$, denoted by solid dots, and $D = 0.2$, denoted by solid crosses. Note that the numerical data are close to the corresponding solid lines, including the $\dot{h} \to 0$ region, lending support to the theoretical hysteresis criterion of Agarwal and Shenoy.

The naive estimates[12] of (2.4), i.e., $T_{P\downarrow}^{-1}(h)$ are also plotted for comparison, as the cross-dashed line $(D = 0.2)$ and dot-dashed line $(D = 0.5)$. Note that in this case for $\dot{h} \to 0$, the naive estimate does not have $\bar{h}_J \to 0$, because the possibility of reverse transition is not taken into account. The simulation values for $D = 0.2$ (solid crosses) and $D = 0.5$ (solid dots) are far away from the corresponding naive estimates. The detailed factors and reverse jumps of the detailed estimate of (2.5) are thus quantitatively important.

Several authors[10,19,24,25] have studied hysteresis for a sinusoidal field sweep $h = H_0 \cos(\Omega t))$, and have sought a "universal" power-law dependence of the hysteresis loop area A with the amplitude H_0 and frequency Ω of the field, namely $A \propto H_0^{\alpha} \Omega^{\beta}$ with α and β independent of H_0, Ω, and D. For a linearly swept field, the "equivalent dependence" is $A \propto \dot{h}^{\gamma}$. However, our numerical simulation result (Fig. 4) does not show this simple power-law dependence, there being no single D-independent exponent γ to fit the data. The hysteresis loop area curve rises steeply for $\dot{h} \simeq 0$, but the rate of variation gets slower and slower (γ fractional) as $\dot{h}$ is increased. The expression (2.8) indicates an initial linear ($\gamma = 1$) $\dot{h}$ dependence for $\dot{h} \to 0$. Within a limited range [0–0.1] of $\dot{h}/h_c$ where a log–log plot can be roughly fitted to a straight line, the slope γ is different for different D. (See Fig. 4, inset, where the data points are from the main figure.)

The hysteresis condition (2.5) implicitly assumes an "adiabatic following" condition with a single "moving-minimum" description of the metastable state. For arbitrarily large $\dot{h}$, this breaks down, as indicated earlier,[15,16] and repeated briefly below.

To observe a well-defined hysteresis the field-sweep rate must be smaller than the relaxation rate T_r^{-1} of the metastable state. Naively, one has[12]

$$T_r^{-1} > \dot{h} \tag{2.9}$$

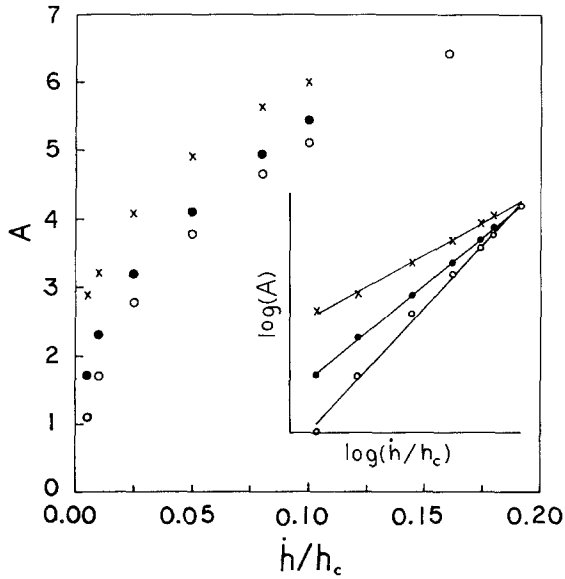

Fig. 4. Area $A(\dot{h})$ of hysteresis loops for $D=0.2$ (crosses $\times$), $D=0.4$ (solid circles $\bullet$), and $D=0.5$ (open circles $\circ$). The inset shows the log–log plots and their least-square linear fits: the slopes or exponents are D dependent.

This condition has been refined[15,16] by noting that in the deterministic field of force, the linearized kinetics is governed by

$$\frac{dm}{dt} = -\frac{\delta\Phi(m)}{\delta m} = -\frac{m-\bar{m}}{T_r}; \qquad \frac{1}{T_r} \equiv \frac{\partial^2\Phi(\bar{m})}{\partial\bar{m}^2}$$

(Noise terms are dropped, as the condition should be valid for any noise strength.) Furthermore,

$$\frac{d\bar{m}(h)}{dt} = \frac{\partial\bar{m}}{\partial h}\dot{h}$$

Therefore, for the system not to deviate appreciably from the metastable minimum as time progresses, we have

$$\frac{d}{dt}(m-\bar{m}) = 0 \qquad \text{for} \quad \frac{m-\bar{m}}{\bar{m}} \ll 1$$

This leads to the condition

$$\dot{h}_{\max} = \frac{1}{T_r}\left[\frac{\partial \ln(\bar{m})}{\partial h}\right]^{-1} > \dot{h} \tag{2.10}$$

Since $T_r^{-1} \to \infty$ as $h \to h_c$, analogous to critical slowing down at the limit of metastability, there must be a breakdown of the inequality close to h_c. For the parameters chosen here, $\dot{h}_{\max}(h)$ would be an almost vertical line in Fig. 3 (not shown), i.e., "good hysteresis" occurs almost up to h_c.

Turning to the diffusion constant (D) dependence, one would expect physically that jumps become enhanced, and the hysteresis loop shrinks, for increasing D with $\dot{h}$ fixed. This can also be seen from the simple form of (2.8). Figure 3 shows such behavior in the data for $D = 0.2$, 0.5 and a given $\dot{h}$. Figure 5 shows $\bar{h}_J(\dot{h}, D)$ values, obtained from numerical simulation, versus D for fixed $\dot{h}/h_c = 0.01$. The data are compared to the theoretical values obtained from the full expression of (2.5). Considering $T_{P\downarrow}^{-1}$ and $T_{P\uparrow}^{-1}$ contributions separately in (2.5), one finds the initial fall of h_J with D is due to the fall of $T_{P\uparrow}^{-1}$, while the leveling off is due to the backward $T_{P\uparrow}^{-1}$ flow contribution becoming significant. [The bars are standard deviations of the stochastic $\{h_J\}$ (non-Gaussian) distribution, and their lengths remain effectively unchanged even if the runs N are made larger.]

Thus the mean jump values $\bar{h}_J(\dot{h})$ lend a fair quantitative support to the theoretical hysteresis window criterion of Agarwal and Shenoy within this simple Landau–Langevin model. It is to be noted that the FPT

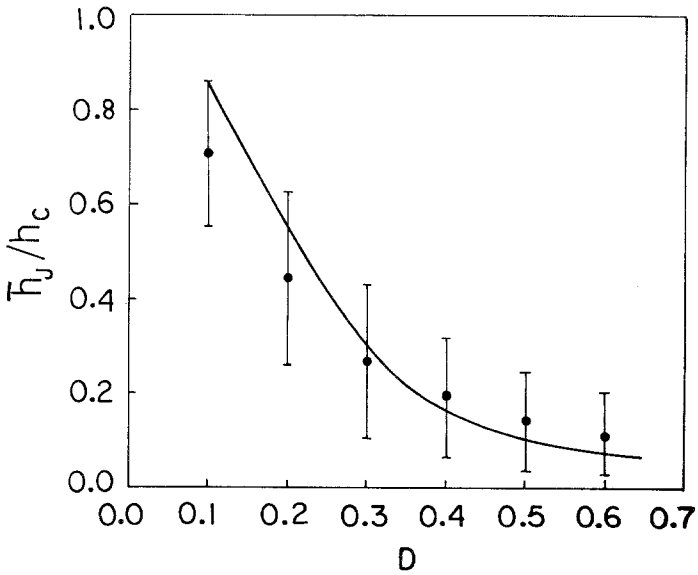

Fig. 5. $\bar{h}_J(\dot{h}, D)$ versus D for fixed $\dot{h} = 0.01\, h_c$ (solid circles ●). Vertical lines show standard deviations of stochastic $\{h_J\}$. The solid line is the theoretical estimate $\dot{h}_{\min}(\bar{h}_J, D)$ of (2.5).

concept is not restricted to the $n=1$ component order parameter, but can be extended[27] to the $\mathbf{m}(\mathbf{r})$ multicomponent/spatially-varying case. The $n=4$ but uniform case was worked out for the two-mode ring laser.[16,28]

3. PASSAGE TIME AND JUMP DISTRIBUTIONS

As is clear from the earlier sections, the passage of the system from one state to the other is driven by noise as well as the external field value. Therefore, the passage times that we record are stochastic, and the corresponding jump field values $\{h_J\}$ follow a distribution $\rho(h_J; \dot{h}, D)$. This distribution, which depends on parameters defining Φ, in addition to $\dot{h}$ and D, is *intrinsically* broad. Figure 6 shows for $D=0.5$ and $\dot{h}/h_c=0.05$ the standard deviation σ_N of h_J from the mean $\bar{h}_J(\dot{h}, D)$ for N repetitions, plotted versus N. Clearly $\sigma_N \to \sigma_\infty \neq 0$. There is a nonzero relative width of scatter of the vertical jumps in Fig. 1 that is intrinsic, and *not* an artefact of insufficient run statistics. The value $N=1000$ typically chosen is already close to the $N \to \infty$ limit. It is thus not sufficient to compare the mean value $\bar{h}_J$ to theoretical estimates; the distribution must be understood as well.

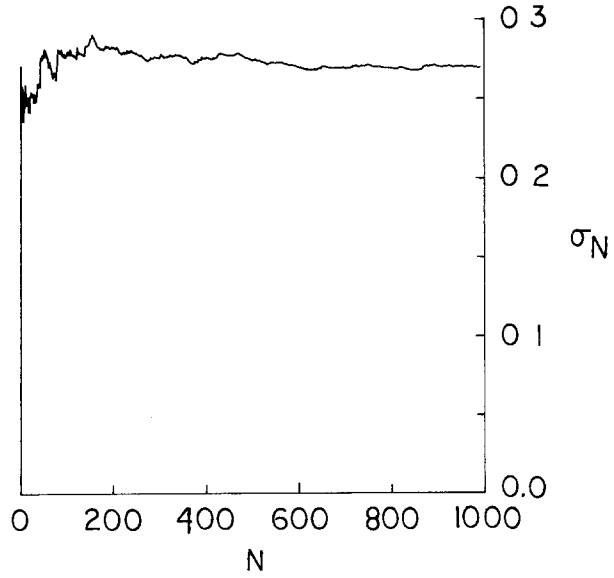

Fig. 6. The standard deviation σ_N about $\bar{h}_J$ of the field jump values $\{h_J\}$ as a function of the number of runs N (see text).

Since a general moving-boundary FPT analysis is not available, we try to understand these distributions using the well-known theoretical fixed-boundary first-passage time distributions $P(\tau)$ in a suitable formulation. For $\dot{h}=0$, in the high-barrier/low-noise limit, $|\Phi(\bar{m}_3)-\Phi(\bar{m}_{1,2})|/D \gg 1$ (valid except close to h_c; refs. 15 and 28), the distributions of first-passage time τ, except in the immediate vicinity of the origin, is exponential[20,16]

$$P(\tau, h) = T_{P\downarrow}^{-1}(h)\, e^{-\tau/T_{P\downarrow}(h)} \tag{3.1}$$

This distribution has been experimentally verified for spontaneous switching in optically bistable ring lasers,[29] and for silica grains hopping in optical traps.[7] It holds[16] also for general order-parameter dimension n. The distribution is broad, but finite moments $\langle \tau^r \rangle = r! \langle \tau \rangle^r$ are finite. In particular, fluctuations $\sigma_\tau \equiv \langle (\tau - \langle \tau \rangle)^2 \rangle^{1/2} / \langle \tau \rangle$ about the mean $T_p = \langle \tau \rangle$ are of order unity.

We need to make the theoretical fixed-boundary distribution relevant for the $\dot{h} \neq 0$ case, in order to derive a valid expression for the h_J distribution. We consider, instead of a linear sweep, very many piecewise constant-field "microsteps" $h_n = h(t_n) = n\dot{h}\Delta$. These steps have time width Δ, connected by vertical "microquenches," and follow the $h(t) = \dot{h}t$ line (Fig. 7). The mean $\bar{h}_J$, obtained previously from a strictly ($h = \dot{h}t$) linear sweep, is virtually unchanged in value in this sequential microquench $h(t)$. The time width Δ is taken sufficiently small so that the time that the system

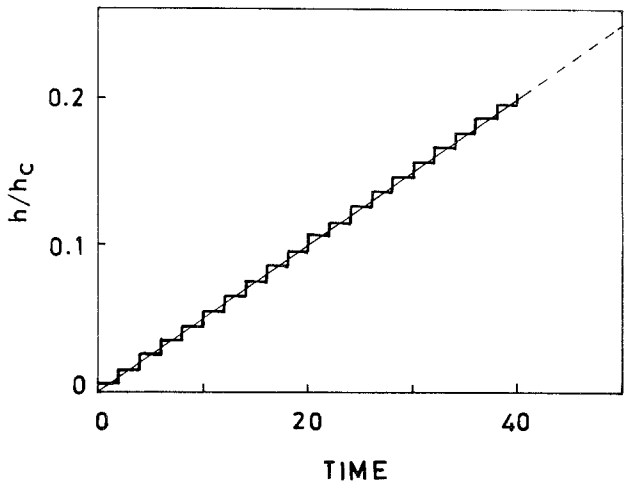

Fig. 7. Field microsteps of time width (thick line) considered in (3.2) to emulate the linear field sweep (thin line) for $\dot{h}/h_c = 0.005$.

takes in the quenched state to roll down (noise effect included) to reach the new metastable minimum is less than 0.1Δ. Thus the system rapidly reequilibrates, and reinitializes to the suddenly changed well minimum at each microquench. Fixed-boundary results[27] can then be safely invoked for each microstep.

The probability density $\rho(h_1; \dot{h})$ for a jump at $h_J = h_1$ in the first constant-h step between $0 < \tau \leqslant \Delta$ is given by $\rho(h_1; \dot{h})\Delta \simeq e^{-\Delta/T_{P\downarrow}(h_1)}(\Delta/T_{P\downarrow}(h_1))$, with $\Delta/T_{P\downarrow} \ll 1$. After the first microquench, the system reequilibrates, and passage attempts begin afresh from a new initial time $t = \Delta$. The probability for passage at the next step $h_J = h_2$ is then

$$\rho(h_2; \dot{h})\Delta \simeq [1 - \rho(h_1; \dot{h})\Delta]\, e^{\Delta/T_{P\downarrow}(h_2)}(\Delta/T_{P\downarrow}(h_2))$$

for times $\Delta < \tau < 2\Delta$. (The prefactor ensures that passage has not previously occurred.) Thus for a jump at $h_J = h_n = n\dot{h}\Delta$,

$$\rho(h_n; \dot{h}) \simeq \left[1 - \sum_{r=1}^{n-1} \rho(h_r; \dot{h})\Delta\right] e^{-\Delta/T_{P\downarrow}(h_n)}/T_{P\downarrow}(h_n) \tag{3.2}$$

and an iterative solution can be obtained numerically for $\rho(h_J; \dot{h})$. Note that the contribution from the reverse jumps is neglected because $T_{P\downarrow}/T_{P\uparrow} \ll 1$ for h not too close to zero.

Figure 8 shows the $\{h_J\}$ histogram (thick solid line) along with the (thin solid line) theoretical distribution (3.2) for $\dot{h} = 0.005 h_c$ and $D = 0.2$. The agreement is good. For example, the theoretical $\bar{h}_J/h_c = 0.33$ for $\dot{h}/h_c = 0.005$ and $D = 0.2$ is within 1% of the numerical simulation histogram-based value. The hump in Fig. 8 arises because of the competition between the falling probability of survival, given by the square bracket of (3.2), and the increasing probability of passage, given by the remaining factors. The distribution broadens for increasing $\dot{h} = 0.01 h_c$, $0.05 h_c$, $0.1 h_c$, with the theoretical curve following the numerical data closely for runs from initial values $h(0) = 0$. (For symmetric forward sweeps from $h(0) = -h_0$ to $h = +h_0$, the theoretical peak occurs somewhat before the histogram value.) The inset shows the $\bar{h}_J$ versus $\dot{h}$ plot of Fig. 3 for $D = 0.2$; now the standard deviation of the stochastic $\{h_J\}$ are also shown. (These are *not* the *error bars* of the numerical experiment in determining $\bar{h}_J$; see Fig. 6. They represent the fact that $\{h_J\}$ is an intrinsically broad distribution in this model.)

As the expression (3.2) is valid only for large times, deviations do occur in Fig. 8 for small $h_J/h_c \ll 1$ for small passage times τ. This might be especially true for larger D values. Figure 9 compares theory and the experimental histogram (for $\dot{h}/h_c = 0.1$) for a relatively large value $D = 0.5$.

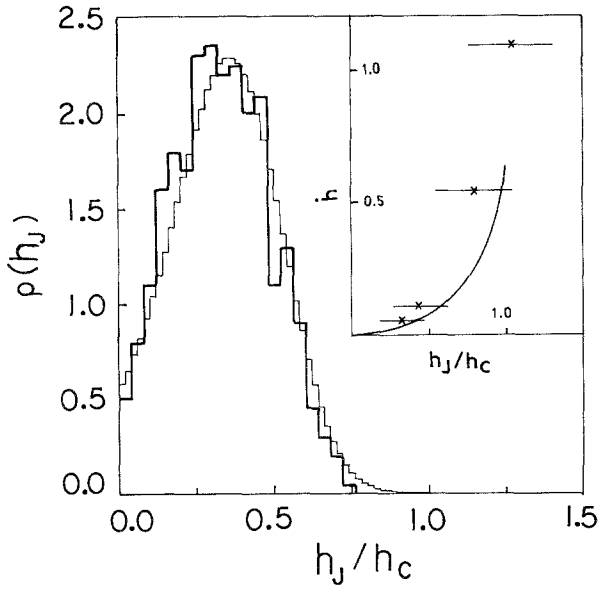

Fig. 8. Comparison of h_J histogram from numerical simulations (thick solid line) with theoretical $\rho(h_J; \dot{h})$ (thin solid) curve for $\dot{h}/h_c = 0.005$ and $D = 0.2$. The microquench steps of $h(t)$ along the $\dot{h} = 0.005\, h_c$ slope line are reflected in the small steps of the thin solid line.

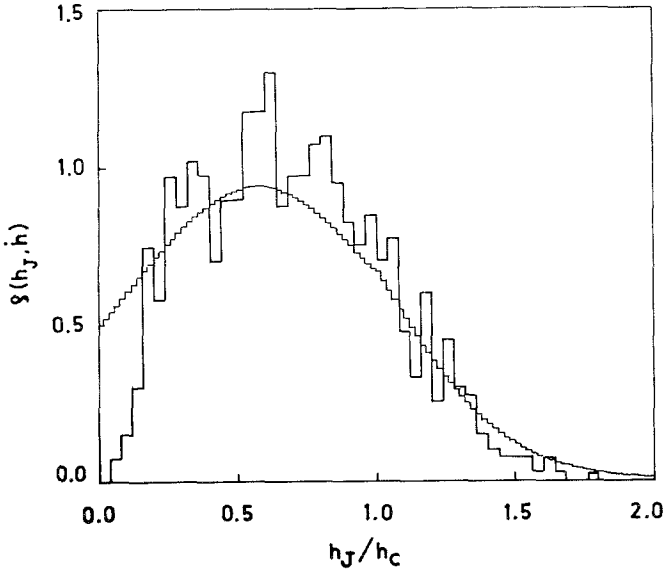

Fig. 9. Same as in Fig. 8, but for $\dot{h}/h_c = 0.1$ and $D = 0.5$.

The mean values $\bar{h}_J/h_c$ from theory and experiment however, differ by only about 5%. Thus $\rho(h_J; \dot{h})$ of (3.2) matches the data quite closely.

Thus the $\{h_J\}$ statistics from numerical simulations can be quantitatively understood reasonably well in terms of a (suitably extended) FPT distribution.

4. SINGLE MAGNETIC DOMAIN MODEL

The uniform-m Landau model clearly ignores many features important in real magnets,[1] such as spatial magnetic domains, coupling anisotropies, etc. However, the model provides a conceptual picture of overshoot phenomena. An interesting aspect of the simulation is the instrinsically broad probability distribution $\rho(h_J; \dot{h})$ of jump fields for repeated sweeps. This at first seems contrary to experience in e.g., magnets, where M–h hysteresis curves are reproducible under fixed cycling conditions. However, a distribution of jump fields has also been invoked in (deterministic) phenomenological models,[5,6] where individual independent domains or "particles" are assumed to have different fields for $-M \to +M$ flips. Characteristic M–h hysteresis loops emerge on spatial averaging over the independent domains. No kinetic or stochastic effects are included in these models. We can consider, however, a collection of *identical* noninteracting finite-volume domains with magnetization described by the uniform-m Landau model and with *stochastic* thermal forces. This is in some sense a picture in the same spirit as the phenomenology of Barker *et al.*,[5,6] but in an opposite conceptual regime. Since the N particles jump independently, spatially averaging during a single sweep will be equivalent to time averaging a single, finite-volume particle over N sweeps. The stochastic jump values $\{h_J\}$ for the single, repeatedly cycled particle obey a jump distribution $\rho(h_J; \dot{h})$. For a field swept in a sawtooth cycle from $h(t) = -h_0$ to $h(t) = +h_0$ and back, the magnetization at a time τ of an ensemble of identical domains is hence

$$M(h(\tau)) = -1 + 2\int_0^\tau \rho(h(t); \dot{h})\dot{h}\, dt \tag{4.1}$$

where the saturation magnetization is taken to be ± 1, and

$$h(t) = -h_0 + \dot{h}t$$

It is interesting to note that for very different reasons, similar ideas of a jump-field distribution [compare (4.1) and Eq. (2) of ref. 5] emerge from the phenomenology.

We plot M versus h in Fig. 10 for various field-sweep rates, diffusion constants $D = 0.2$, 0.5, and the ρ distribution from simulations, to check the qualitative shape of the hysteresis curve. The characteristic double-beaked M versus h curve emerges. Hysteresis is disfavored by larger D, as seen by comparing Figs. 10a and 10b: the loop area is reduced.

An extension of these single-domain rate competition ideas to models with intergrain coupling or domain size variation would require solving

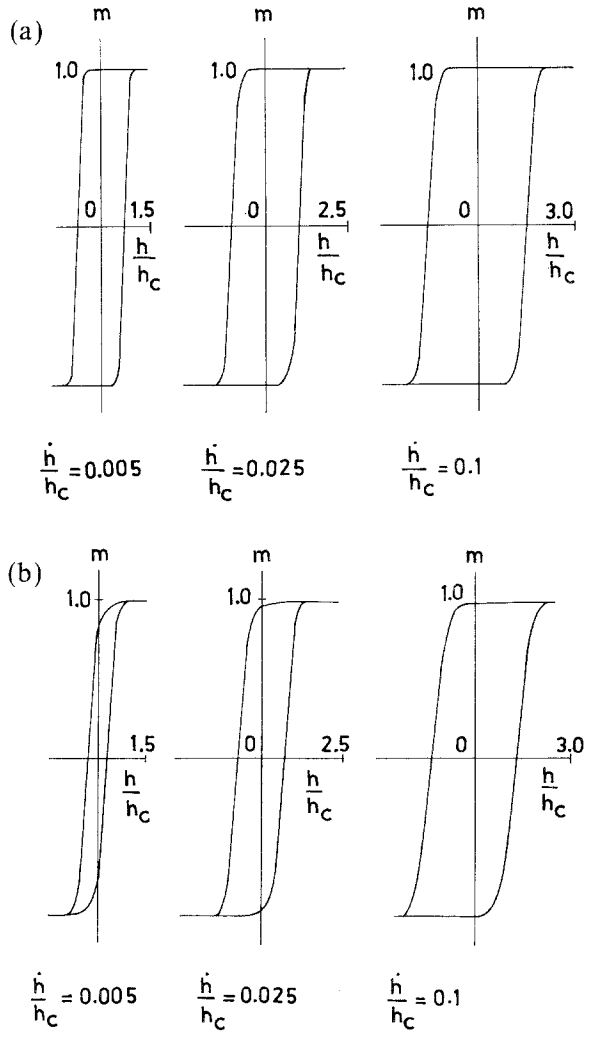

Fig. 10. Hysteresis loops obtained from numerical simulations at sweep rates $\dot{h}/h_c = 0.005$, 0.025, and 0.1 for (a) $D = 0.2$ and (b) $D = 0.5$.

coupled Langevin equations for $\{m_i\}$, which would be difficult. However, even this simple model yields qualitatively reasonable M–h curves, indicating that the extension of rate competition ideas to more realistic magnetic models might be worth pursuing.

5. DISCUSSION

We have performed numerical simulations of Langevin dynamics of a simple Landau model. A previous first-passage-time-based hysteresis criterion[15,16] for the mean jump field $\bar{h}_J(\dot{h}, D)$ is shown to be quantitatively validated in regard both to the field-sweep-rate and diffusion-constant dependence. The fluctuations in h_J are also shown to be understood in terms of the FPT fluctuations. Thus a *quantitative* understanding of hysteresis is obtained within the conceptual framework of rate competition ideas for this simple model.

Further work could include the consideration of a linearly swept $h(t)$ and hysteresis in the master equation-based mean-field model of Paul *et al.*[23] The extension of the hysteresis criterion to realistic models in quantum optics, magnetism, and glasses requires a consideration of multicomponent and spatially varying order parameters. The key quantity is the mean first-passage time, which can be expressed in terms of multicomponent integrals over the stationary distributions $P_0(\mathbf{m}) = e^{-\Phi(\mathbf{m})/D}$. The theoretical framework (FPT) is not restricted to single-component order parameters.[27,16] A calculation of the hysteresis window for the two-mode ring laser with a four-component order parameter $[E_{1x}, E_{1y}; E_{2x}, E_{2y}]$ has already been done.[16] Further numerical work could include a simulation of the ring laser Langevin equation[29] with a linearly swept pump parameter $a(t) = a_1(t) - a_2(t) = a(0) + \dot{a}t$ or cosine time dependence.[4] An experimental check of hysteresis in real ring lasers with spontaneous switching between two modes,[4,29] but for constant rate $\dot{a} \neq 0$, would be of much interest. Similarly, a linearly swept double-well optical trap of the silica grain[17] would be a direct check of the theoretical predictions of (2.6) and Figs. 4, 5 and Figs. 8, 9.

For condensed matter systems, in magnetism or glassy systems, spatially varying order parameters $\rho(\mathbf{r})$ (e.g., the density) enter, which correspond to an infinite number of components. The first-passage time would then be a functional integral over $e^{-\Phi(\rho(\mathbf{r}))/D}$. An example of a $\Phi(\rho(\mathbf{r}))$ model functional is the density-functional formalism of Ramakrishnan and Yussouff,[30] which describes liquid-to-crystal transitions or glassy states. In the context of critical cooling rates in glasses, Uhlman[3] has considered plots of melt-to-crystal transformation time versus temperature ($T-T-T$ curves). These can be reexpressed as *rates* (inverse FPT) versus the critical

control parameter, temperature, and interpreted as a particular shape of hysteresis window boundary.

Another class of problems include the effects on hysteresis of colored noise,[31] which can be generated by external sources in laser systems, for example. Theoretically, this would be handled by calculating the FPT for a delta-correlated model in one higher dimension. Simulations are underway.[32] One might further consider a full back-and-forth sweep sawtooth $h(t)$, with $\dot{h}$ piecewise constant, to understand stochastic-synchronization-like effects[17,33] in the FPT rate competition picture. Preliminary simulations[32] show a series of diminishing peaks of jump fields (or times) similar to experiment.[17] We hope to report on some of these applications elsewhere.

In summary, we have numerically simulated the Langevin dynamics of a simple finite-volume Landau model, and found supporting evidence for a theoretical hysteresis criterion based on rate competition, and with a broad, but theoretically understandable distribution of stochastic jump values. These ideas could have relevance in magnetic hysteresis and glassy supercooled systems.

APPENDIX

The numerical solution[34] of the stochastic differential equation (2.1) involves a time discretization $t \to t_n = n\delta t$ and a choice of a random force value from a Gaussian distribution[35] (constant) within each time step of size δt. Since the equation is nonlinear, the choice of δt is crucial to get results of reasonable accuracy. The physically correct solution would be to take $\delta t \to 0$: time is continuous. However, as the value of δt is reduced, the computer time spent to integrate between two given points increases, limiting accessibility of small δt values. This we see by repeating the experiment of Suzuki[36] for a system to roll down the potential surface (2.2) (with $h = 0$, $\dot{h} = 0$) from the unstable point to either of the equivalent minima for various δt values. The computer time with $\delta t \to 0$ increases rapidly. For example, with the same initial seed value for the random number generator (for example, -2) for $\delta t = 0.01$, 0.001, and 0.0001 the CPU-times in MicroVax II were 38, 99, and 437 sec, respectively. The trajectories followed in all the three cases (in the m–t plane) are also different. Since we are following a stochastic process, which involves averages over many runs, the results are not conclusive unless we can fix δt physically and remove arbitrariness in the choice. The criterion we adopt, therefore, is to choose a value of δt so as to match theoretically calculated ($\delta t = 0$) mean first-passage times to within a specified accuracy. This δt is then used in the hysteresis simulations.

The mean first-passage time T_P of a random viarable is known from solving a Fokker–Planck based differential equation.[20] The initial, $t=0$, value $m(t)=m(0)$ is in an "inside" region Ω, and it moves randomly to meet the boundary $\partial\Omega$ in a random time τ. For $m(t)$ a single component (as in our case), an exact solution[15,20] for $T_P=\langle\tau\rangle$ from $m=m_{\text{initial}}$ (in our case $\bar{m}_1$) to $m=m_{\text{final}}$ ($\bar{m}_3$, for example) is

$$T_p = -\int_{\bar{m}_3}^{\bar{m}_1} \frac{dm''}{DP_0(m'')} \int_{-\infty}^{m''} dm'\, P_0(m') \tag{A.1}$$

where

$$P_0(m) = e^{-\Phi(m)/D} \tag{A.2}$$

This is easily evaluated for various values of h in (2.2), and provides a good check on our numerical simulation result. For the general (n-component) case the FPT expression is also an (n-component) integral over the stationary distribution.[27,16]

The mean FPTs are evaluated for various h values from the computer simulation of (2.1) for passage from $\bar{m}_1$ to $\bar{m}_3$ for various values of δt over many repeated runs. The number of runs taken was such that the fluctuation of the mean FPT is brought to about 1%. In Fig. 11 we show the variation

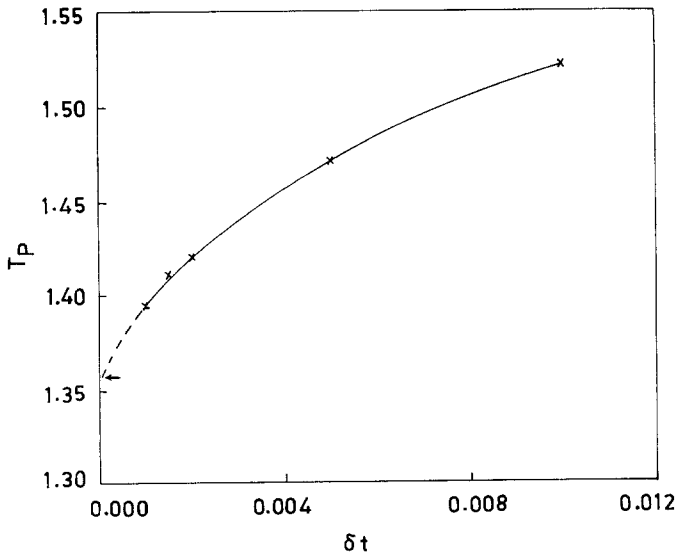

Fig. 11. Numerically simulated T_P for $\dot{h}=0$, $h/h_c=0.9$, and $D=0.2$ as a function of discretization time unit δt. The theoretical value ($\delta t \to 0$) is shown on the T_P axis by an arrow.

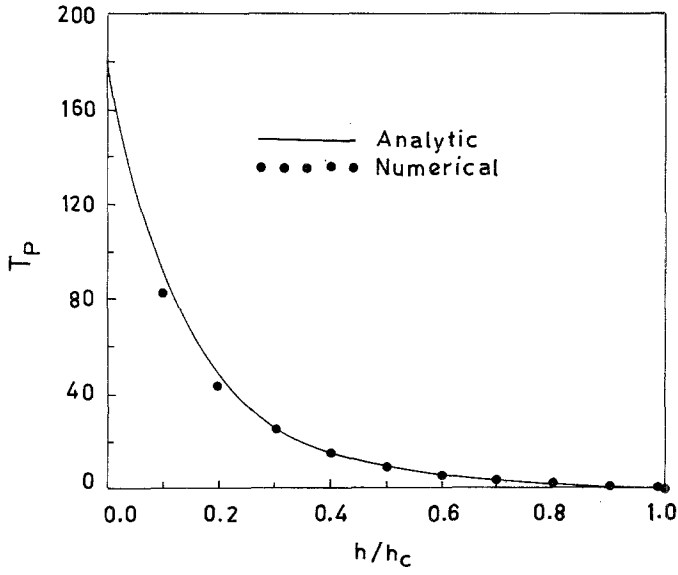

Fig. 12. Comparison of numerically simulated $T_P(h)$ (●) with ($\delta t = 0.001$) with the theoretical values (solid line) for which $\delta t = 0$. The passage boundary is taken to be the peak of the free-energy barrier.

of the simulated mean FPT with δt. Note that the curve converges toward the theoretical value on extrapolation to $\delta t = 0$ (the theoretical value marked by an arrow). As a compromise between the loss of accuracy and affordable computer run time, we choose $\delta t = 0.001$ in our calculation, for which the difference between simulated and theoretical mean FPT values remains well below 5% for almost the entire range [0, 1] of h/h_c. For better comparison we plot in Fig. 12 the theoretical and numerically simulated mean FPT values for $\delta t = 0.001$ and h/h_c in the range [0, 1]. We see that the comparison is very good except close to $h/h_c = 0$ and $h/h_c = 1$. Close to $h/h_c = 0$ the deviations ($\sim 10\%$) occur because (A.1) does not account for the reverse passage $\bar{m}_3 \to \bar{m}_1$. The deviations close to $h/h_c = 1$ occur because in this test calculation we choose the absorbing boundary to be the unstable maximum ($\bar{m}_3$) of the potential Φ, and the mean FPT becomes comparable to δt as the barrier vanishes. This last problem does not appear in our main calculation because there we choose the final boundary point to be the stable minimum ($\bar{m}_2$), so that T_P is always much larger than δt.

Thus the exact expression for the mean FPT serves as a benchmark to fix the discretization step $\delta t = 0.001$ in hysteresis simulations.

ACKNOWLEDGMENTS

It is a pleasure to thank L. Turski and R. Balian for valuable references, G. S. Agarwal for useful conversations, and the Department of Science and Technology (India) and University Grants Commision (India) for partial support.

REFERENCES

1. S. Chikazumi, *Physics of Magnetism* (Wiley, New York, 1964).
2. M. Avrami, *J. Chem. Phys.* **7**:1103 (1939).
3. D. R. Uhlman, *J. Non-cryst. Solids* 7:337 (1972).
4. E. G. Gage and L. Mandel, *J. Opt. Soc. Am. B* **6**:287 (1989).
5. J. A. Barker, D. E. Schreiber, B. G. Huth, and D. H. Everett, *Proc. R. Soc. Lond. A* **386**:251 (1983).
6. W. F. Brown, *J. Appl. Phys.* **33**:1308 (1962).
7. E. P. Wohlfarth, *J. Appl. Phys.* **35**:783 (1964).
8. I. D. Mayergoyz, *Phys. Rev. Lett.* **56**: 1518 (1986).
9. G. F. Mazenko and M. Zannetti, *Phys. Rev. B* **32**:4565 (1985).
10. M. Rao, H. R. Krishnamurthy, and R. Pandit, *Phys. Rev. B* **42**:856 (1990).
11. V. P. Skriprov and A. V. Skiprov, *Sov. Phys. Usp.* **22**:389 (1979).
12. R. Gilmore, *Phys. Rev. A* **20**:2510 (1979).
13. D. Kumar, in *Proceedings of the Winter School in Stochastic Processes, Hyderabad, 1982* (Springer, Berlin 1983), p. 186.
14. C. P. Bean, *J. Appl. Phys.* **26**:1381 (1955).
15. G. S. Agarwal and S. R. Shenoy, *Phys. Rev. A* **23**:2719 (1981).
16. S. R. Shenoy and G. S. Agarwal, *Phys. Rev. A* **28**:1315 (1984).
17. A. Simon and A. Libchaber, *Phys. Rev. Lett.* **68**:3375 (1992).
18. M. C. Mahato and S. R. Shenoy, in Proceedings of International Workshop on Statistical Physics of Solids and Glasses, Calcutta, December, 1991, *Physica A* **186**:220 (1992).
19. M. Acharyya, B. K. Chakrabarti and A. K. Sen, *Physica A* **186**:231 (1992); W. S. Lo and R. A. Pelcorits, *Phys. Rev. A* **42**:7471 (1990).
20. R. Stratonovich, *Topics in the Theory of Random Noise*, (Gordon and Breach, New York, 1963), Vol. 1, Chapter 4.
21. H. A. Kramers, *Physica C* 7:284 (1940).
22. K. Binder, *Rep. Prog. Phys.* **50**:783 (1987).
23. W. Paul, D. W. Heermann, and K. Binder, *J. Phys. A* **22**:3325 (1989).
24. S. Sengupta, Y. J. Marathe, and S. Puri, *Phys. Rev. B* **45**:7828 (1992).
25. D. Dhar and P. B. Thomas, *J. Phys. A* **25**:4967 (1990); *Europhys. Lett.* **21**:965 (1993).
26. P. Jung, G. Gray, R. Roy, and P. Mandel, *Phys. Rev. Lett.* **65**:1873 (1990).
27. Z. Schuss and B. J. Matkowsky, *SIAM J. Appl. Math.* **35**:604 (1979); Z. Schuss, *SIAM J. Rev.* **22**:119 (1980).
28. K. P. N. Murthy and S. R. Shenoy, *Phys. Rev. A* **36**:5087 (1987).
29. R. Roy, R. Short, J. Durnin, and L. Mandel, *Phys. Rev. Lett.* **45**:1486 (1980).
30. T. V. Ramakrishnan and M. Yussouff, *Phys. Rev. B* **19**:2775 (1979); A. D. J. Haymet and D. W. Oxtoby, *J. Chem. Phys.* **74**:2559 (1981); C. Dasgupta, unpublished.

31. F. Moss and P. V. E. McClintock, eds., *Noise in Nonlinear Dynamical Systems* (Cambridge University Press, Cambridge, 1989).
32. B. Chattopadhyay, M. C. Mahato, and S. R. Shenoy, unpublished.
33. P. Jung and P. Hanggi, *Phys. Rev. A* **44**:8033 (1991); *Europhys. Lett.* **8**:505 (1989), and references therein.
34. D. W. Heermann, *Computer Simulation Methods in Theoretical Physics* (Springer-Verlag, Berlin, 1986).
35. W. H. Press, B. P. Flannery, S. A. Teukolsky, and W. T. Vetterling, *Numerical Recipes* (Cambridge University Press, Cambridge, 1987).
36. M. Suzuki, *Adv. Chem. Phys.* **46**:195 (1981).